RSC Advances

PAPER

View Article Online
View Journal | View Issue

Cite this: *RSC Adv.*, 2026, **16**, 11521

Exploring the grafting copolymer of CNF-*graft*-PHEMA as a coating for packaging paper

Noverra Mardhatillah Nizardo, *[a] Naifa Inayah Hadiana,[a] Chaulah Achyar,[a] Aniek Sri Handayani,[b] Azzah Dyah Pramata,[c] Mukti Zainuddin[d] and Annisa Rifathin[e]

Received 19th November 2025
Accepted 20th January 2026

DOI: 10.1039/d5ra08935b

rsc.li/rsc-advances

Packaging materials are essential for protecting commodities from external environmental factors and ensuring their quality during transportation. Food and beverage products, such as fresh milk, fish, and meat, require packaging that prevents spoilage. In this study, CNF surfaces were modified to enhance hydrophobicity *via* free radical graft copolymerization using 2-hydroxyethyl methacrylate (HEMA) as a monomer and cerium ammonium nitrate (CAN) as an initiator. The resulting CNF-*graft*-PHEMA was isolated to remove homopolymers using DMF : methanol as the solvent. The isolation time and DMF : methanol ratio were varied to optimize the purity of the produced graft copolymer. Based on the viscosity and degree of grafting, the optimum conditions for CNF-*graft*-PHEMA were found to be a DMF : methanol ratio of 2 : 1 and an isolation time of 48 h. CNF-*graft*-PHEMA/cellulose acetate composites were prepared at varying cellulose acetate (CA) concentrations to evaluate their impact on the coating barrier properties *via* WVTR and water contact angle measurements. Based on the results of the WVTR and water contact angle tests, CNF-*graft*-PHEMA/CA 5 wt% exhibited an improvement in barrier properties, with a WVTR value of 1.6198 g m^{-2} 4 h and a water contact angle of 104.67°.

1 Introduction

Packaging materials are crucial for storing and protecting products from external environmental influences and for ensuring that they reach consumers in good condition.[1] The delivery of food and beverage products, such as fresh milk, fish, and meat, from producers to consumers requires a low-temperature packaging system to minimize product loss due to spoilage.[2]

The use of single-use packaging materials for food delivery, such as EPS and PU, has recently raised environmental concerns due to increasing waste accumulation. To mitigate plastic waste accumulation in the environment, researchers have been developing biodegradable and sustainable materials as alternatives to single-use packaging plastics, such as cellulose-based packaging materials.[3] Notably, a comparative environmental life cycle assessment of cellulose nanofiber films based on synthetic polymers used in packaging was reported by Nadeem *et al.*, who concluded that the environmental impacts could be lowered in comparison to synthetic packaging.[4] However, cellulose-based packaging materials have limitations owing to their poor mechanical and barrier properties; thus, they require further modification.[5]

Cellulose acetate (CA) is one of the most interesting cellulose derivatives due to its biodegradability and high optical transparency, making it suitable for film packaging applications.[6] CA is synthesized *via* the acetylation of cellulose using an excess of acetic anhydride in the presence of a sulfuric acid catalyst. The biodegradability of cellulose acetate (CA) depends on its degree of acetylation; CA with a low acetylation or substitution degree (below 2.5) is capable of degradation. Given these benefits, CA, along with CNF, can be considered a promising biodegradable plastic material that could serve as an alternative to fossil-based plastic.[7] As reported in the literature, along with cellulose, CA has been studied owing to its potential as an active packaging material.[8,9]

In 2022, Singh *et al.* developed a hydrophobic paper made from cellulose fibers coated with modified lignin and cellulose acetate. The results of this study demonstrated that the coated paper had a water contact angle greater than 130°, indicating a significant improvement in hydrophobicity compared to the uncoated paper. Furthermore, the water vapor transmission rate (WVTR) of the paper was significantly reduced, indicating that this coating also improved the moisture barrier of the

[a]*Department of Chemistry, Faculty of Mathematics and Natural Sciences, University of Indonesia, Kampus UI, Depok, 16424, Indonesia. E-mail: noverra.mardhatillah@sci.ui.ac.id*

[b]*Department of Chemical Engineering, Faculty of Engineering, Indonesian Institute of Technology, South Tangerang City, 15314, Indonesia*

[c]*Department of Materials and Metallurgical Engineering, Faculty of Industrial Technology and System Engineering, Institut Teknologi Sepuluh Nopember, Kampus ITS Sukolilo, Surabaya 60111, Indonesia*

[d]*Faculty of Marine Science and Fisheries, Universitas Hasanudin, Makasar, Sulawesi Selatan, Indonesia*

[e]*Research Center for Polymer Technology, National Research and Innovation, PUSPIPTEK Area, South Tangerang, Indonesia*

paper.[10] In addition, Pieters and Mekonnen created a Pickering emulsion using cellulose acetate as the dispersed phase, air as the continuous phase, and CNC as a stabilizer to maintain emulsion stability for application as an environmentally friendly paper coating. The resulting paper coating demonstrated improved oil resistance and air permeability within the coating. Furthermore, the Cobb value for air permeability in the paper showed a 60% increase.[11] Chen *et al.* in 2024 successfully modified cellulose acetate (CA) reinforced with TEMPO–CNF as a coating, exhibiting better mechanical properties and optical qualities than pure cellulose acetate coatings.[12] These studies have shown that the modification of cellulose-based materials as coating materials can be an alternative for plastics, water-based paints, coatings, and applications that require transparent materials.[13]

Our previous studies reported the graft copolymerization of HEMA and DMAEMA onto CNF and used it as a coating on paper packaging. The results confirmed an improvement in the mechanical and barrier properties of the coated paper with an acceptable viscosity.[14] Nevertheless, the purity of the resulting CNF-*graft*-PHEMA and the optical transparency of the coated paper still need to be improved. In this respect, we attempted to fill this research gap by presenting our work, which lies in optimizing CNF-*graft*-PHEMA and preparing CNF-*graft*-PHEMA/CA and studying its performance as a coating on paper. To the best of our knowledge, there have been no prior reports on the potential applications of CNF-*graft*-PHEMA/CA composite coatings on paper. Based on the above statement, this study attempts to examine the use of chemically modified cellulose nanofibrils (CNFs) in smart packaging. In this research article, CA was modified with cellulose nanofibril-*graft*-poly(2-hydroxyl methacrylate) (CNF-*graft*-PHEMA) to improve the mechanical and barrier properties of CA coating materials. CNF-*graft*-PHEMA was synthesized by grafting CNF with an HEMA monomer. The isolation process of the graft copolymers was conducted by varying the isolation time and the ratio of DMF to methanol to determine the highest purity of CNF-*graft*-PHEMA. Moreover, CNF-*graft*-PHEMA was mixed with various concentrations of CA to determine the optimum barrier properties of the CNF-*graft*-PHEMA/CA composites. The synthesized CNF-*graft*-PHEMA/CA composites were characterized using Fourier transform infrared (FTIR) spectroscopy to analyze the functional groups and a viscometer to determine their viscosity. Afterwards, the composites were applied to paper as a coating, and the performance of the paper coated with composites was tested for grammage, water vapor transmission rate (WVTR), and water contact angle.

2 Experimental section

2.1. Materials

Oil palm empty fruit bunch (OPEFB), distilled water, acetone, sodium hydroxide (NaOH), glacial acetic acid (CH_3COOH), sodium chlorite ($NaClO_2$), nitric acid (HNO_3), cerium ammonium nitrate (CAN), 2-hydroxyethyl methacrylate (HEMA), dimethylformamide (DMF), ethanol, methanol and commercial cellulose acetate ($M_n \sim 30\,000$ g mol^{-1} with acetyl content of 38.9 wt%).

2.2. Synthesis of micro-fibrillated cellulose (MFC)

MFC was extracted from an oil palm empty fruit bunch (OPEFB) using a multi-step bleaching process. The OPEFB (500 g) was soaked in 10 liters of distilled water for 24 hours, followed by washing the OPEFB using 5 liters of distilled water and 5 liters of acetone. Then, the OPEFB was dried in an oven at 60 °C for 36 hours, and the particle size was reduced with a 100 mesh sieve. After that, 150 g of sifted OPEFB was mixed with 4 wt% NaOH on a hot plate at 80 °C for 3 hours, followed by washing and filtering until a neutral pH was achieved. This process was repeated three times. The OPEFB was then bleached by mixing it with an acetate buffer solution (40.5 g NaOH, 112.5 mL glacial acetic acid, and 1500 mL H_2O) on a hot plate at 80 °C for 2 hours, followed by washing and filtering until the pH was neutral. Afterwards, the OPEFB was mixed with a solution of 1.7% $NaClO_2$ at 80 °C for 2 hours, followed by washing and filtering until a neutral pH was obtained. The bleaching process was repeated three times. The obtained MFC was dried in an oven at 40 °C for 36 hours.

2.3. Synthesis of cellulose nanofibril (CNF) 2%

To obtain 2% of CNF, 40 g of MFC was added to 1960 mL of distilled water and stirred with an Ultra-Turrax for 8 hours at 20 000 rpm with a cycle of 10 minutes off and 10 minutes on. Subsequently, the MFC was sonicated using ultrasonic Hielscher for 5 minutes with a cycle of 10 seconds on and 10 seconds off. The total sonication time was 90 min.

2.4. Synthesis of CNF-*graft*-PHEMA

Graft copolymerization was performed using the method developed by Littunen *et al.*, with some modifications.[15] First, the pH of a 2 wt% CNF suspension was adjusted to 1 using nitric acid, followed by bubbling nitrogen gas through the suspension. After 15 min of stirring, CAN was added as the catalyst. Subsequently, 30 mmol of HEMA was added gradually to the mixture and stirred continuously for 30 min at 35 °C.

2.5. Isolation of the graft copolymer

The polymer isolation process was conducted to separate the homopolymer from the graft copolymer. Briefly, 1 g of CNF-*graft*-PHEMA was dispersed in 50 mL of acetone and stirred for 15 min, followed by filtration to collect the precipitate. The graft copolymer isolation process was carried out by adding DMF :

Table 1 Variation in the isolation time

Test number	Time (hours)
1	12
2	24
3	48
4	60

Table 2 Variations in the isolation solvent ratio

Solvent ratio composition		
DMF : methanol (v : v)	Methanol (mL)	DMF (mL)
1 : 0	60	0
2 : 1	40	20
1 : 1	30	30
1 : 2	20	40
0 : 1	0	60

Table 3 Variations in cellulose acetate concentrations

Composition	
CNF-*graft*-PHEMA (g)	Cellulose acetate (wt%)
1	0
1	5
1	10
1	15

methanol into the precipitate and heating it in a Soxhlet apparatus at 160 °C. The variations in isolation time and the ratio of DMF : methanol as solvent to CNF-*graft*-PHEMA isolation are shown in Tables 1 and 2. Afterwards, the CNF-*graft*-PHEMA precipitate was purified by redissolving the graft copolymer in methanol, filtering to remove impurities, and then drying in an oven at 50 °C. This method was adapted from the work of Nishioka *et al.*[16]

2.6. Homogenization with cellulose acetate

The CNF-*graft*-PHEMA/CA composite was synthesized by mixing CNF-*graft*-PHEMA and CA, as adapted from the work of Cindradewi *et al.*[17] First, 1 g of CNF-*graft*-PHEMA and CA was dispersed in acetone and stirred at room temperature for 2 hours. The mixture was then ultrasonicated at 25 °C for 3 minutes, followed by pouring into a polystyrene Petri dish and drying in an oven at 40 °C for more than one day. The variations in the cellulose acetate concentrations used for the synthesis of the CNF-*graft*-PHEMA/cellulose acetate composite are shown in Table 3.

2.7. CNF-*graft*-PHEMA/cellulose acetate composite coating on paper

The coating process using the bar coating method was carried out based on the research of Nizardo *et al.*[18] In the bar coater machine, the paper was clamped, and the bar coater was installed. Then, the CNF-*graft*-PHEMA/CA composite was poured onto the paper, and the machine was run for one pass until the coating was evenly distributed. The coating process was carried out using bar coater sizes of 4, 8, 25, and 60 μm. Next, the paper was dried in an oven at 40 °C until it was completely dry.

2.8. Characterization

The CNF-*graft*-PHEMA/CA composite was characterized using FTIR to investigate the functional groups formed during the synthesis process, calculate the viscosity, and determine the degree of grafting (DoG). The CNF-*graft*-PHEMA/cellulose acetate-coated paper was tested using several methods to evaluate its performance as packaging. Water vapor resistance was tested by measuring the water vapor transmission rate (WVTR). To investigate the hydrophobicity of the coated paper, water was dripped onto the coated paper, and the contact angle was then measured.

2.8.1. FTIR. The sample was mixed with KBr powder by grinding and put into a pellet-forming mold before being placed in the FTIR sample holder. The FTIR spectrum was recorded using a PerkinElmer 1760-X FTIR spectrometer ranging from 4000 to 400 cm^{-1} with a resolution of 0.5 cm^{-1}.

2.8.2. Degree of grafting (DoG). The measurement of the degree of grafting of CNF-*graft*-PHEMA was calculated using the peak height of the C=O group produced through FTIR characterization using the following equation:

$$\text{Degree of grafting} = \frac{\%\ \text{transmittance product}}{\%\ \text{transmittance HEMA}} \times 100\%. \quad (1)$$

2.8.3. Viscometry. Viscosity measurements of the samples were performed using a Thermo Scientific Haake viscometer. A liquid sample of 100–150 mL was poured into a container. A spindle of the required type and size was then installed, and the rotational speed (RPM) of the viscometer was adjusted. The viscosity value shown on the display was recorded.

2.8.4. Particle size. The PSA measurement procedure was carried out by placing the sample in the form of an aqueous dispersion in a cuvette, which is then inserted into the PSA holder.

2.8.5. WVTR. The test was conducted by weighing a 4 × 4 cm piece of coated paper. Then, 10 mL of distilled water was poured into a plastic container and covered with coated paper. The container with the paper lid was placed in a desiccator and tightly closed. The coated paper used as the cover was weighed every hour, and this step was repeated four times.

2.8.6. SEM. The morphologies of MFC and CNF were studied using a field emission scanning electron microscope (FE-SEM) (Apreo 2 SEM, Thermo Fisher Scientific Inc., United States) at an accelerating voltage of 2.00 kV. The CNF sample was obtained by freeze drying the 2% CNF suspension. Before the observation, the samples were coated with gold.

3 Results and discussion

3.1. Synthesis of MFC

MFC was synthesized from the OPEFB as the source of cellulose through delignification and bleaching processes. These processes aim to separate cellulose from other lignocellulose components. A pretreatment process was carried out to produce a high degree of cellulose content. The bleaching process was carried out to increase the purity of cellulose by washing the OPEFB with distilled water and acetone, which aimed to clean

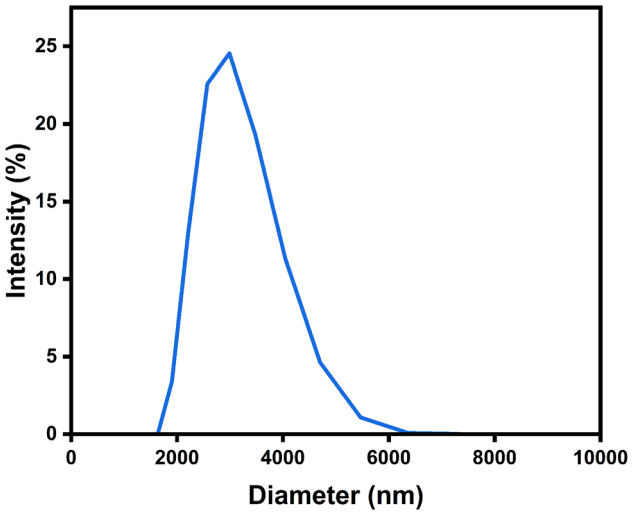

Fig. 1 Particle size distribution of MFC.

the surface of the OPEFB from any contaminants.[19] The delignification process was performed using NaOH solution to remove lignin and hemicellulose and to remove the remaining lignin residue.[20] This bleaching process was carried out in two stages: the first stage used an acetate buffer solution, and the second stage used a solution of 1.7% sodium chlorite as a bleaching agent. $NaClO_2$, owing to its highly oxidative properties, can selectively oxidize lignin residues without causing significant damage to the cellulose polymer chain.[21] MFC was characterized using a particle size analyzer (PSA) to measure the distribution of the particle size. Fig. 1 shows that the cellulose particles in MFC have an average *Z* size of 3149 nm, with a polydispersity index of 0.09542. The obtained MFC diameters were smaller than those reported by Spence *et al.*, who synthesized MFC with diameters of 1–10 μm *via* high-pressure homogenization without chemical pretreatment.[22] Delignification and bleaching processes to remove lignin from the fibers produced MFCs with a more uniform diameter.[23]

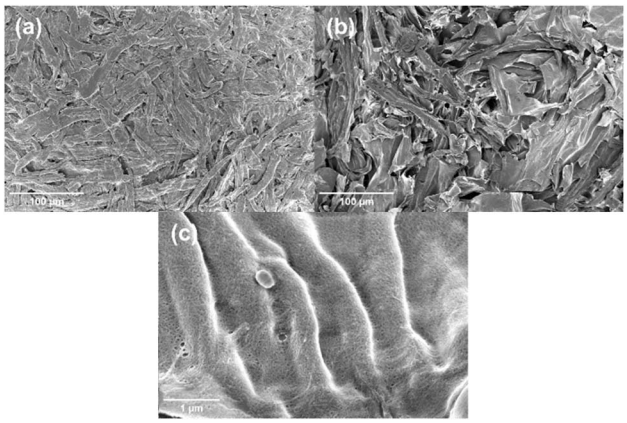

Fig. 3 FE-SEM images of MFC (a), CNF at 1000× magnification (b) and 750 00× magnification (c).

3.2. Synthesis of 2% CNF

The 2% CNF synthesis process was conducted through homogenization and sonication processes. The homogenization process was performed using an Ultra-Turrax homogenizer to homogenize, disperse, and emulsify the cellulose suspension.[22] The sonication process was carried out by sonicating the diluted MFC for 90 min to break down the agglomeration of microscopic particles, producing a more stable and uniform dispersion of CNF.[24] The synthesized CNFs were characterized by PSA to determine the particle size distribution. Fig. 2 shows that 1% CNF 1% and 2% CNF had average *Z* sizes of 2106 nm and 311.7 nm, and polydispersity indices of 0.894 and 0.5022, respectively. Based on the obtained particle size, the particle diameter of 2% CNF is smaller and more uniform than that of 1% CNF, as higher CNF concentrations allow more fibrils in the suspension to form a stronger and more stable network, resulting in a more uniform particle distribution.[25] Although the particle diameters did not reach the typical nanocellulose size (<100 nm),[18] 2% CNF was selected based on these results.

Furthermore, the FE-SEM images in Fig. 3 confirmed the formation of CNF, showing the morphological differences between MFC and the resulting CNF. The MFC exhibited

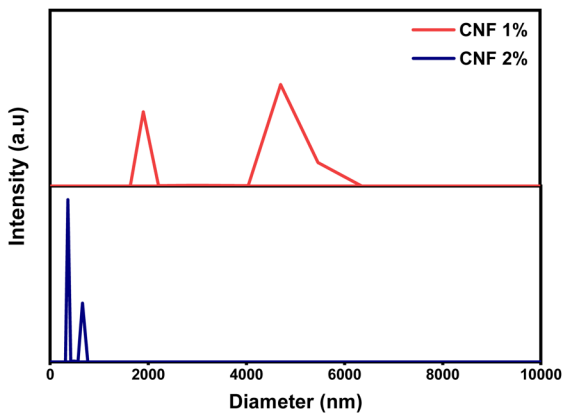

Fig. 2 Particle size distribution of 1% CNF and 2% CNF.

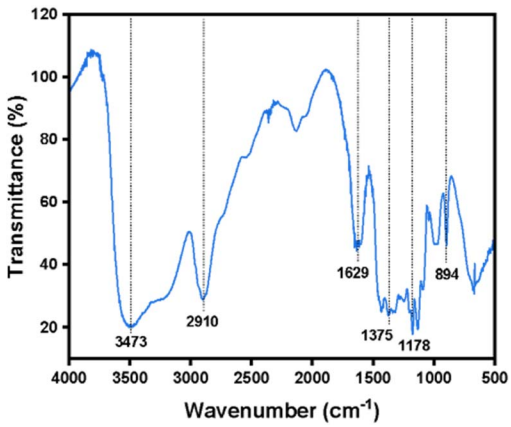

Fig. 4 FTIR spectra of 2% CNF.

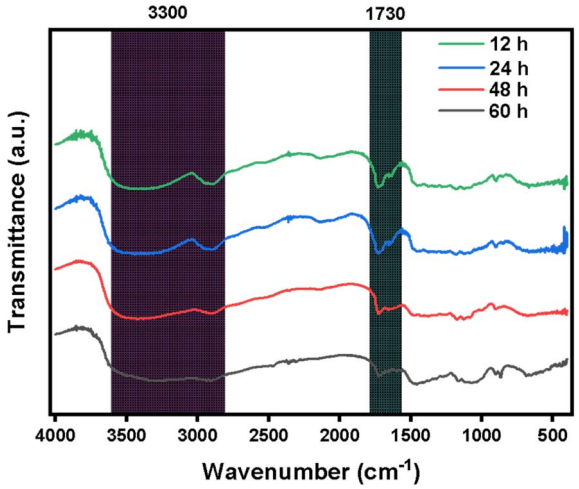

Fig. 5 FTIR spectra of CNF-*graft*-PHEMA isolation time variation.

cellulose fibers with diameters in the micrometer range, while the CNF sample no longer displayed discrete micrometer-scale fibers; instead, it showed a sheet-like morphology. This morphology might be due to fiber wall delamination during mechanical processing.[26] At 750 00× magnification, a partially fibrillated network was visible, indicating that fiber delamination had occurred. However, the extent of fibrillation was not sufficient to fully individualize the cellulose microfibrils into a nanofibrillar network.

The 2% CNF was characterized by FTIR to analyze the functional groups. The FTIR results in Fig. 4 show the presence of O–H longitudinal vibrations at 3473 cm^{-1} and C–H longitudinal vibrations at 2910 cm^{-1}. The stretching vibrations of O–H and C=O at 1629 cm^{-1} are attributed to the absorbed water molecules and hydroxymethyl (CH_2OH) groups. The C–O stretching and bending vibrations at 1178 cm^{-1} and 1375 cm^{-1}, respectively, correspond to the cellulose backbone. The absorption peak at 894 cm^{-1} corresponds to the presence of β glycosidic bonds.[27] These results confirm that 2% CNF had the characteristic structure of cellulose.

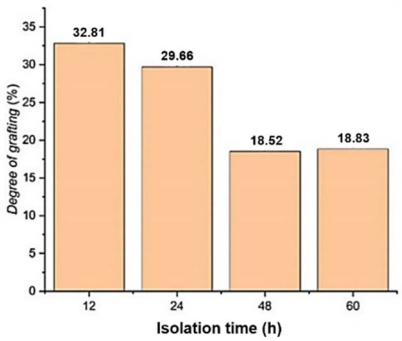

Fig. 6 Effect of isolation time on the degree of grafting CNF-*graft*-PHEMA.

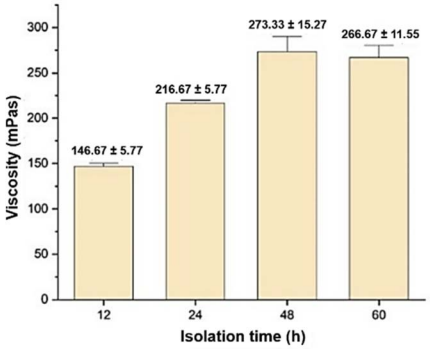

Fig. 7 Effect of isolation time on CNF-*graft*-PHEMA viscosity.

3.3. Optimization isolation time of CNF-*graft*-PHEMA

To separate the homopolymer from the graft copolymer, the isolation process of CNF-*graft*-PHEMA was conducted to obtain high purity CNF-*graft*-PHEMA.[16] The isolation process was carried out using the Soxhlet extraction method with methanol as the solvent, followed by the characterization of the isolated CNF-*graft*-PHEMA using FTIR. The FTIR results in Fig. 5 show that after the isolation process, CNF-*graft*-PHEMA had lower intensity absorption peaks for O–H stretching and C=O vibration at 3300 cm^{-1} and 1730 cm^{-1}, respectively. Fig. 6 shows the DoG values for CNF-*graft*-PHEMA at different isolation times. The minimum DoG value (18.52%) was achieved after 48 h of isolation. This is supported by the FTIR results, revealing reduced C=O absorption at 1730 cm^{-1} due to the dissolution of PHEMA homopolymer carbonyl groups during the isolation process. Longer isolation times enable more selective and thorough separation of homopolymers, yielding higher purity CNF-*graft*-PHEMA.[28] Fig. 7 shows the viscosity of each CNF-*graft*-PHEMA at various isolation times, with 48 h isolation yielding the highest CNF-*graft*-PHEMA viscosity (273.4 mPa s). This agrees with previous results showing that the homopolymers (PHEMA and CNF) dispersed thoroughly during 48 h of isolation. Consequently, pure graft copolymers with larger, more complex structures dominate, increasing their viscosity.[29]

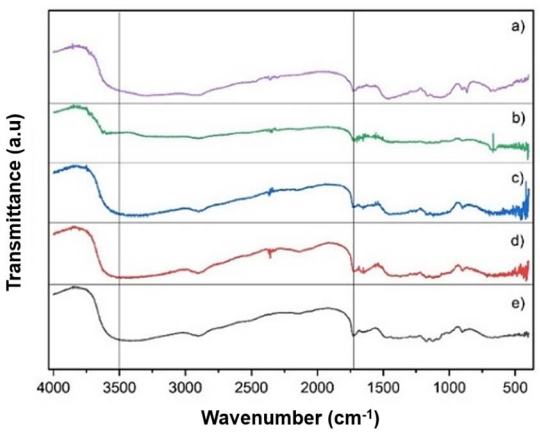

Fig. 8 FTIR spectra of isolated CNF-*graft*-PHEMA variations in DMF : methanol solvent ratio: (a) 1 : 0 ratio, (b) 2 : 1 ratio, (c) 1 : 1 ratio, (d) 1 : 2 ratio, and (e) 0 : 1 ratio.

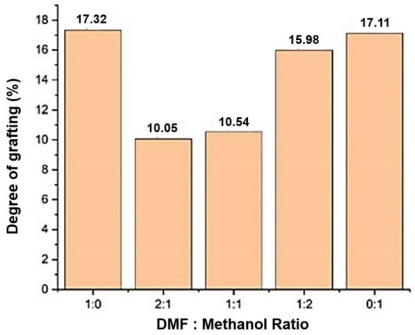

Fig. 9 Effect of the ratio of the isolation solvent on the degree of grafting of CNF-*graft*-PHEMA.

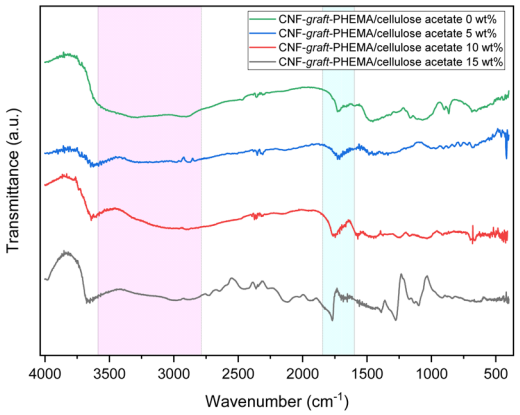

Fig. 11 Spectra FTIR CNF-*graft*-PHEMA/CA.

However, viscosity decreased after 60 h of isolation due to the incomplete removal of homopolymers and residual monomers, which prevented the optimal formation of the CNF-*graft*-PHEMA graft structure.[30] These results indicate that the optimum isolation time for CNF-*graft*-PHEMA is 48 h. The optimum isolation time was also confirmed through statistical analysis, in which the isolation time had a significant effect on viscosity (one-way ANOVA, $p < 0.001$), with the highest value observed at 48 h, which was significantly higher than those at 12 and 24 h, but did not differ significantly from that at 60 h.

3.4. Optimization isolation solvent ratio of CNF-*graft*-PHEMA

To determine the optimum DMF : methanol ratio for producing high purity CNF-*graft*-PHEMA, various synthesized graft copolymers were characterized. DMF is a polar aprotic solvent with the ability to break the hydrogen bonds between the PHEMA homopolymer and the CNF backbone. Methanol can dissolve the PHEMA homopolymer without degrading the CNF backbone.[31] The FTIR characterization results in Fig. 8 show that all CNF-*graft*-PHEMA at different DMF : methanol ratios exhibited a decrease in the intensity of the C=O and O–H vibration peaks at 1730 cm^{-1} and 3300 cm^{-1}, respectively. These results show that free PHEMA and CNF homopolymers were dissolved at different DMF : methanol ratios, yielding a high-purity graft copolymer.[16] The DoG results of CNF-*graft*-PHEMA produced at different DMF : methanol ratios are shown in Fig. 9. A DMF : methanol ratio of 2 : 1 showed a decrease in the DoG value due to a decrease in the intensity of the C=O peak, verifying that the PHEMA homopolymer was completely dissolved.[16] Fig. 10 shows the viscosity measurement results of the CNF-*graft*-PHEMA produced at different solvent ratios. The solvent ratio of 2 : 1 produced the highest viscosity at 290 mPa s. The increased CNF-*graft*-PHEMA viscosity after isolation using a DMF : methanol ratio of 2 : 1 was due to the properties of DMF, a polar aprotic solvent with a high dipole moment that solvated the polymer chains, thus reducing interchain interactions and preventing aggregation.[32]

Meanwhile, methanol facilitated CNF-*graft*-PHEMA deposition by enhancing cellulose solubility, yielding a high-purity graft copolymer with more complex chain entanglements that increased flow resistance and solution viscosity.[33] Analyzing the results, the isolation solvent ratio had a significant effect on viscosity (one-way ANOVA, $p < 0.001$), with the highest value observed for the 2 : 1 solvent ratio. This was significantly higher than those from 1 : 1, 1 : 2, and 0 : 1 ratios but did not differ significantly from the 1 : 0 ratio.

3.5. Homogenization with cellulose acetate

To enhance the mechanical properties of CNF-*graft*-PHEMA as a coating material, various concentrations of CA were mixed

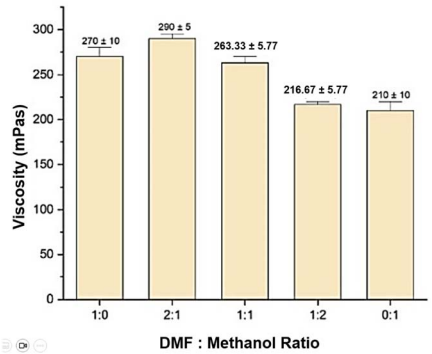

Fig. 10 Effect of the isolation solvent ratio on CNF-*graft*-PHEMA viscosity.

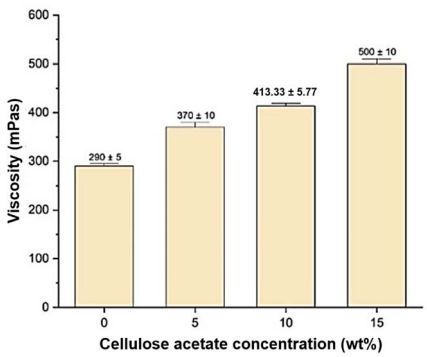

Fig. 12 Effect of cellulose acetate concentration on the viscosity of the CNF-*graft*-PHEMA/CA composites.

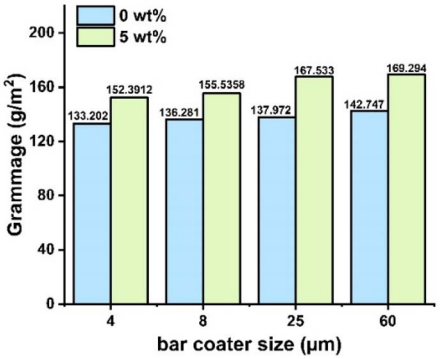

Fig. 13 Effect of bar coater size on the grammage of the paper coated with CNF-*graft*-PHEMA/CA.

with the graft copolymer *via* a homogenization process to obtain the optimum mechanical properties of the produced CNF-*graft*-PHEMA/CA composites. The homogenization aimed to enhance the properties of the composite as a coating material by reducing water vapor and gas permeability and increasing the tensile strength and tear resistance of the coated paper.[34] The synthesized CNF-*graft*-PHEMA/CA composites were characterized by FTIR to evaluate the formed functional groups. The FTIR spectra in Fig. 11 showed a decreasing intensity of the absorption peaks of O–H and C=O at 3300 cm^{-1} and 1730 cm^{-1}, respectively, after the incorporation of CA into the graft copolymer. The O–H and C=O groups in the CNF were replaced by acetyl ($–COCH_3$) groups from CA, with peak intensities increasing with higher CA concentrations.[35]

3.6. Coating performance of CNF-*graft*-PHEMA/cellulose acetate on food packaging paper

The viscosity of the respective CNF-*graft*-PHEMA/CA composites was investigated before studying the coating performance of the CNF-*graft*-PHEMA/CA composites. The high viscosity of coating materials can reduce water permeability by increasing the layer thickness.[36] Viscosity measurements in Fig. 12 revealed that CNF-*graft*-PHEMA/CA composite viscosity increased with CA concentration, resulting in a rigid chain structure of CA.[37] The optimal viscosity for paper coating applications (200–400 mPa s)[38] was obtained at 5 wt% CA (370 mPa s). In this respect, viscosity measurements showed that there was a strong positive correlation between CNF-*graft*-PHEMA/CA composite viscosity and CA concentration ($r(10) = 0.989$, $p < 0.001$).

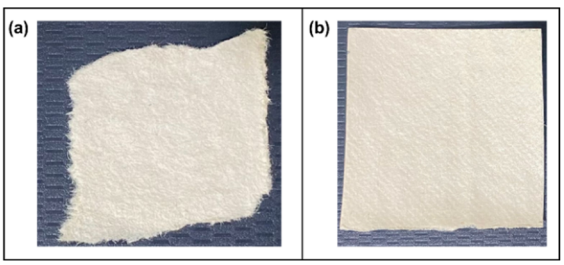

Fig. 14 Images of the (a) uncoated paper and (b) coated paper using a bar coater size of 25 μm.

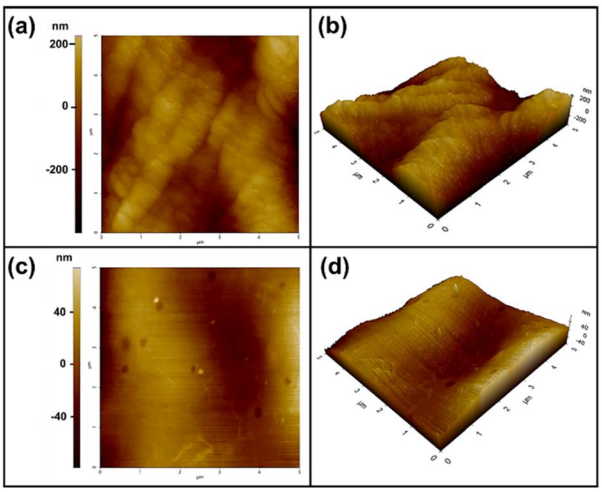

Fig. 15 AFM images of (a and b) uncoated paper and (c and d) coated paper using a bar coater size of 25 μm.

The CNF-*graft*-PHEMA/CA composite obtained with cellulose acetate addition concentrations of 0% and 5% was coated on paper using different sizes of bar coater to explore its potential application as a packaging paper coating. Based on Fig. 13, it was found that the larger the size of the bar coater used, the greater the coating grammage or coating thickness produced. Moreover, the coating thickness on the paper can affect the smoothness and mechanical properties of the coating material and provide a higher adhesion strength value. Furthermore, Fig. 14 shows an image of the non-coated paper and the coated paper. To observe more clearly the coating performance of the CNF-*graft*-PHEMA/CA composite, AFM measurement was conducted. The non-coated paper features native cellulose fibers with some microfibrils on their surface, as shown by the AFM pictures in Fig. 15. In addition, the AFM images of coated papers with CNF-*graft*-PHEMA/CA composite are typically smoother and introduce a nanoscale roughness while entirely covering the microscale roughness of the paper substrate.

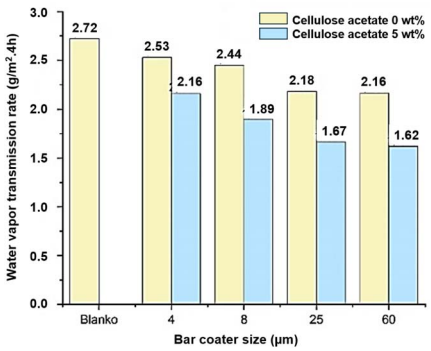

Fig. 16 WVTR test results of the CNF-*graft*-PHEMA/CA composite coatings.

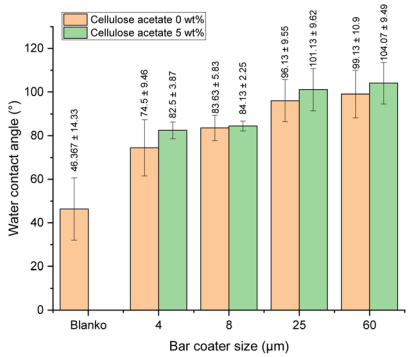

Fig. 17 Water contact angle of paper with the CNF-*graft*-PHEMA/CA composite coating.

3.7. Water vapor transmission rate test (WVTR) of coated packaging paper

The WVTR of coated paper was determined to study the moisture barrier properties of the CNF-*graft*-PHEMA/CA composite as a coating material.[22] Fig. 16 shows that the composite-coated paper exhibited lower WVTR values than the uncoated paper. Higher bar coater sizes additionally reduced WVTR by increasing the coating thickness, thereby enhancing the barrier to water vapour.[39] Optimal WVTR for the CNF-*graft*-PHEMA/CA composite coating was achieved at 5 wt% CA using a 60 μm bar coater. Although a decreasing trend in WVTR with increasing bar coater size was observed, the linear relationship was not statistically significant ($p > 0.05$). Consistently, one-way ANOVA showed no significant differences in WVTR among the different bar coater sizes ($p > 0.05$).

3.8. Water contact angle test of coated packaging paper

The water contact angle of the coated paper was also studied, and the results are shown in Fig. 17. Water contact angle measurements show that the coated paper exhibits greater hydrophobicity (contact angle > 70°) than the uncoated paper (46.37°), indicating that the uncoated paper tends to exhibit hydrophilic properties and is easier to moisten with water.[40] The CNF-*graft*-PHEMA/CA coating displayed higher hydrophobicity than neat CNF-*graft*-PHEMA, demonstrating that the composite enhanced the hydrophobicity of the packaging paper more effectively.

4 Conclusions

In conclusion, CNF-*graft*-PHEMA was successfully synthesized *via* Soxhlet extraction using DMF : methanol at a ratio of 2 : 1 for 48 h. In addition, the higher the isolation time, the higher the viscosity that can be obtained while decreasing DoG. The addition of CA onto CNF-*graft*-PHEMA enhanced the overall viscosity of the composites and paper barrier properties, with a WVTR value of 1.62 g m^{-2} 4 h and a water contact angle of 104.67° at a concentration of 5 wt% and a bar coater of 60 μm. Further studies are needed to explore its potential as a smart packaging material.

Author contributions

Noverra Mardhatillah Nizardo contributed to conceptualizing the research, data analysis, and interpretation, reviewing and editing the original draft, and funding acquisition. Naifa Inayah Hadiana conducted experiments, characterized the products, and wrote the original draft of the manuscript. Chaulah Achyar contributed to data analysis and editing. Aniek Sri Handayani designed the methodology for coating and performance tests and data interpretation and reviewed and edited the original draft. Azzah Dyah Pramata and Mukti Zainuddin reviewed and edited the original draft. Annisa Rifathin contributed to data analysis.

Conflicts of interest

There are no conflicts to declare.

Data availability

The authors confirm that the data supporting the findings of this study are available within the article.

Acknowledgements

The authors acknowledge Universitas Indonesia for the research funding of Riset Kolaborasi Indonesia (RKI) under funding year of 2025, with contract number PKS-630/UN2.RST/HKP.05/2025. The authors acknowledge the Integrated Laboratory and Research Center (ILRC), Universitas Indonesia and the Badan Riset dan Inovasi Nasional (BRIN) for the characterization facilities. Notably, the authors thank Green Polymer Technology Research Group at the Department of Metallurgical and Material Engineering, Universitas Indonesia, for facilitating the water contact angle analysis.

References

1 P. Jackson and V. Viehoff, *Appetite*, 2016, **98**, 1–11, DOI: 10.1016/J.APPET.2015.11.032.
2 R. Montanari, *Trends Food Sci. Technol.*, 2008, **19**, 425–431, DOI: 10.1016/J.TIFS.2008.03.009.
3 B. Schumann and M. Schmid, *Innov. Food Sci. Emerg. Technol.*, 2018, **47**, 88–100, DOI: 10.1016/J.IFSET.2018.02.005.
4 H. Nadeem, P. Nimmegeers, W. Batchelor and P. Billen, *Food Bioprod. Process.*, 2024, **145**, 175–186, DOI: 10.1016/j.fbp.2024.03.005.
5 C. L. Reichert, E. Bugnicourt, M. B. Coltelli, P. Cinelli, A. Lazzeri, I. Canesi, F. Braca, B. M. Martínez, R. Alonso, L. Agostinis, S. Verstichel, L. Six, S. De Mets, E. C. Gómez, C. Iißbrücker, R. Geerinck, D. F. Nettleton, I. Campos, E. Sauter, P. Pieczyk and M. Schmid, *Polymers*, 2020, **12**, 1558, DOI: 10.3390/POLYM12071558.
6 N. R. Saha, G. Sarkar, I. Roy, A. Bhattacharyya, D. Rana, G. Dhanarajan, R. Banerjee, R. Sen, R. Mishra and

D. Chattopadhyay, *RSC Adv.*, 2016, **6**, 92569–92578, DOI: 10.1039/C6RA17300D.
7 S. Fischer, K. Thümmler, B. Volkert, K. Hettrich, I. Schmidt and K. Fischer, *Macromol. Symp.*, 2008, **262**, 89–96, DOI: 10.1002/MASY.200850210.
8 V. Bugatti, G. Viscusi and G. Gorrasi, *Foods*, 2020, **9**, 1414, DOI: 10.3390/foods9101414.
9 A. Jayakrishnan, S. Shahana and R. Ayswaria, *RSC Sustain.*, 2024, **2**, 2335–2347, DOI: 10.1039/D3SU00450C.
10 S. S. Singh, A. Zaitoon, S. Sharma, A. Manickavasagan and L. T. Lim, *Int. J. Biol. Macromol.*, 2022, **223**, 1243–1256, DOI: 10.1016/J.IJBIOMAC.2022.11.066.
11 K. Pieters and T. H. Mekonnen, *Mater. Today Chem.*, 2024, **42**, 102370, DOI: 10.1016/J.MTCHEM.2024.102370.
12 H. Chen, G. Hou, K. Chitbanyong, M. Takeuchi, I. Shibata and A. Isogai, *React. Funct. Polym.*, 2024, **205**, 106083, DOI: 10.1016/J.REACTFUNCTPOLYM.2024.106083.
13 Y. Chen, B. Geng, J. Ru, C. Tong, H. Liu and J. Chen, *Cellulose*, 2018, **25**, 895, DOI: 10.1007/S10570-017-1553-X/METRICS.
14 N. M. Nizardo, A. N. Saffanah, A. F. Salsabila, A. A. Putri, A. S. Handayani, A. I. Pangesty and M. Chalid, *J. Renewable Mater.*, 2025, **0**, 1–10, DOI: 10.32604/jrm.2025.02024-0068.
15 K. Littunen, U. Hippi, L. S. Johansson, M. Österberg, T. Tammelin, J. Laine and J. Seppälä, *Carbohydr. Polym.*, 2011, **84**, 1039–1047, DOI: 10.1016/J.CARBPOL.2010.12.064.
16 N. Nishioka, T. Yumen, Y. Matsumoto, K. Monmae and K. Kosai, *Polym. J.*, 1986, **18**, 323–330, DOI: 10.1295/POLYMJ.18.323.
17 A. W. Cindradewi, R. Bandi, C. W. Park, J. S. Park, E. A. Lee, J. K. Kim, G. J. Kwon, S. Y. Han and S. H. Lee, *Polymers*, 2021, **13**, 2990, DOI: 10.3390/POLYM13172990.
18 N. M. Nizardo, N. A. D. Sugandi and A. S. Handayani, *Polym.-Plast. Technol. Mater.*, 2024, **63**, 447–458, DOI: 10.1080/25740881.2023.2291435.
19 L. Pudjiastuti, T. Widjaja, A. Altway, I. Rohmania and N. A. Rohmah, *AIP Conf. Proc.*, 2021, **2349**(1), 020062, DOI: 10.1063/5.0052179.
20 G. Chinga-Carrasco, N. Kuznetsova, M. Garaeva, I. Leirset, G. Galiullina, A. Kostochko and K. Syverud, *J. Nanopart. Res.*, 2012, **14**(12), 1280, DOI: 10.1007/S11051-012-1280-Z.
21 S. W. Gadzama, O. K. Sunmonu, U. S. Isiaku and A. Danladi, *Sci. World J.*, 2020, **15**, 100–105.
22 K. L. Spence, R. A. Venditti, O. J. Rojas, Y. Habibi and J. J. Pawlak, *Cellulose*, 2010, **17**, 835–848, DOI: 10.1007/S10570-010-9424-8.
23 M. Jonoobi, R. Oladi, Y. Davoudpour, K. Oksman, A. Dufresne, Y. Hamzeh and R. Davoodi, *Cellulose*, 2015, **22**, 935–969, DOI: 10.1007/S10570-015-0551-0/METRICS.
24 H. Delmas and L. Barthe, *Power Ultrasonics: Applications of High-Intensity Ultrasound*, 2015, pp. 757–791, DOI: 10.1016/B978-1-78242-028-6.00025-9.
25 G. Albornoz-Palma, D. Ching, A. Andrade, S. Henríquez-Gallegos, R. T. Mendonça and M. Pereira, *Polymers*, 2022, **14**, 3843, DOI: 10.3390/POLYM14183843/S1.
26 D. Klemm, F. Kramer, S. Moritz, T. Lindström, M. Ankerfors, D. Gray and A. Dorris, *Angew. Chem., Int. Ed.*, 2011, **50**, 5438–5466, DOI: 10.1002/anie.201001273.
27 S. S. Lal and S. T. Mhaske, *Cellulose*, 2019, **26**(10), 6099–6118, DOI: 10.1007/S10570-019-02509-7.
28 M. Sadeghi and H. Hosseinzadeh, *J. Chil. Chem. Soc.*, 2010, **55**, 497–502, DOI: 10.4067/S0717-97072010000400019.
29 M. N. Obaid, S. M. Hassan and A. Alabadi, *E3S Web Conf.*, 2025, **627**, 03002, DOI: 10.1051/E3SCONF/202562703002.
30 Y. Guo, R. Song, R. Feng, G. Dai, Y. Liang, D. Pu, X. Zhang and Z. Ye, *J. Appl. Polym. Sci.*, 2019, **136**, 47051, DOI: 10.1002/APP.47051.10974628.
31 S. Naz, N. Ahmad, J. Akhtar, N. M. Ahmad, A. Ali and M. Zia, *IET Nanobiotechnol.*, 2016, **10**, 395–399, DOI: 10.1049/IET-NBT.2015.0116.
32 S. Kim, D. Lee and H. Kim, *Gels*, 2024, **10**, 607, DOI: 10.3390/GELS10090607/S1.
33 B. Briscoe and P. Luckham, *Polymer*, 2000, **41**, 3851–3860, DOI: 10.1016/S0032-3861(99)00550-9.
34 Y. Liu, S. Ahmed, D. E. Sameen, Y. Wang, R. Lu, J. Dai, S. Li and W. Qin, *Trends Food Sci. Technol.*, 2021, **112**, 532–546, DOI: 10.1016/J.TIFS.2021.04.016.
35 E. Huda, R. Rahmi and K. Khairan, *IOP Conf. Ser. Earth Environ. Sci.*, 2019, **364**, 012021, DOI: 10.1088/1755-1315/364/1/012021.
36 K. Mohammed, D. Yu, A. A. Mahdi, L. Zhang, M. Obadi, W. Al-Ansi and W. Xia, *Int. J. Biol. Macromol.*, 2024, **259**, 129383, DOI: 10.1016/J.IJBIOMAC.2024.129383.
37 F. H. Kusumah, I. Sriyanti, D. Edikresnha, M. M. Munir and K. Khairurrijal, *Mater. Sci. Forum*, 2017, **880**, 95–98, DOI: 10.4028/WWW.SCIENTIFIC.NET/MSF.880.95.
38 D. W. Bousfield and A. Co, *Rheology Series*, 1999, vol. 8, pp. 827–842, DOI: 10.1016/S0169-3107(99)80009-4.
39 F. Fahrullah, D. Kisworo, B. Bulkaini, W. Yulianto, B. R. D. Wulandani, H. Haryanto, A. Noersidiq, V. Maslami, K. Ulkiyah, K. Kartika and L. Rahmawati, *J. Iimu-Ilmu Peternak.*, 2024, **34**, 11–20, DOI: 10.21776/UB.JIIP.2024.034.01.02.
40 M. A. Hubbe, D. J. Gardner and W. Shen, *Bioresources*, 2015, **10**, 8657–8749, DOI: 10.15376/BIORES.10.4.8657-8749.